Near infrared in vivo measurements of photosystem I and its lumenal electron donors with a recently-developed spectrophotometer

Ginga Shimakawa, Pierre Sétif, Anja Krieger-Liszkay

[#]**Corresponding Author:** Ginga Shimakawa

Institute for Integrative Biology of the Cell (I2BC), CEA, CNRS, Université Paris-Sud, Université Paris-Saclay, 91198 Gif-sur-Yvette cedex, France

E-mail: ginshimakawa@gmail.com

Title: Near infrared *in vivo* measurements of photosystem I and its lumenal electron donors with a recently-developed spectrophotometer

Authors: Ginga Shimakawa[#], Pierre Sétif and Anja Krieger-Liszkay
Institute for Integrative Biology of the Cell (I2BC), CEA, CNRS, Université Paris-Sud, Université Paris-Saclay, 91198 Gif-sur-Yvette cedex, France

Conflict of Interest: The authors declare that they have no conflict of interest.

Abstract

In photosynthesis research, non-invasive *in vivo* spectroscopic analyses have been used as a practical tool for studying photosynthetic electron transport. Klas-NIR spectrophotometer has been recently developed by Klughammer and Schreiber (2016) for *in vivo* measurements of redox changes of P700, plastocyanin (Pcy) and ferredoxin (Fd). Here we show examples using the Klas-NIR spectrophotometer for the evaluation of the redox states and quantities of these components in plant leaves and cyanobacterial suspensions. The redox poise under light of the electron transport components is different in leaves from higher plants compared with cyanobacteria. During a short illumination with an actinic light, P700, Pcy, and Fd are kept reduced in barley leaves but are oxidized in cyanobacteria. During far-red light illumination, P700 and Pcy are mostly oxidized in the leaves but are partially kept reduced in cyanobacteria. In the cyanobacterium *Thermosynechococcus elongatus*, which has no Pcy but uses cytochrome c_6 (cyt c_6) as the electron donor to photosystem I, a cyt c_6 signal was detected *in vivo*. To show the potential of Klas-NIR spectrophotometer for studying different developmental stages of a leaf, we performed measurements on fully mature and early senescing barley leaves. Pcy content in leaves decreased during senescence at an early stage. The Pcy loss was quantitatively analyzed using Klas-NIR spectrophotometer, giving absolute ratios of Pcy to PSI of 2.5 and 1.6 in younger and older leaves, respectively. For quantification of the signals *in vivo*, *in vitro* data (Sétif et al. 2019) obtained with Klas-NIR spectrophotometer were used.

Keywords: Photosynthesis; Photosystem I; Plastocyanin; Cytochrome c_6; Ferredoxin; Leaf senescence

Introduction

Photosystem I (PSI), the large protein complex in the thylakoid membrane in all oxygenic photoautotrophs, plays the important role in the photosynthetic electron transport system to oxidize and reduce in the light the soluble electron carriers plastocyanin (Pcy) and ferredoxin (Fd) on the donor and acceptor sides, respectively. Light excitation of the reaction centers of photosystem II (PSII) and PSI leads to the formation of $P680^+$ and $P700^+$, respectively, and triggers photosynthetic linear electron transport from PSII to PSI through plastoquinone, the cytochrome (cyt) b_6f complex, and Pcy. In this process, O_2 and H^+ are generated at PSII on the luminal side of the thylakoid membrane, and H^+ is also imported from the stroma to the lumen by the Q-cycle in the cyt b_6f complex. The proton

gradient across the thylakoid membrane together with an electrochemical gradient function as the motive force for producing ATP by the chloroplast ATP synthase. On the electron acceptor side of PSI, Fd is reduced via the chlorophylls A_0, the phylloquinones A_1, and the iron-sulfur clusters F_X, F_A, and F_B. Finally, $NADP^+$ is reduced to NADPH by the Fd-$NADP^+$ reductase. Both NADPH and ATP are utilized for photosynthetic CO_2 assimilation in the stroma of chloroplasts (the so-called Calvin-Benson cycle). In some cyanobacteria, like *Thermosynchecoccus elongatus* (*T. elong.*) Pcy is replaced by cyt c_6 independent of the growth conditions while in most species Pcy is the main electron donor under normal growth conditions but can be replaced by cyt c_6 upon cupper deficiency.

Non-invasive spectroscopic analysis in the near infrared region is an important tool to evaluate the *in vivo* redox states and the quantities of electron transport cofactors and partners of PSI. Originally, it has been established that the redox state of P700 can be obtained from the transmittance difference in the near infrared region (Harbinson and Woodward 1987; Schreiber et al. 1988). *In vivo* spectroscopic analysis combined with a saturation pulse light method has led to the definition of the effective quantum yield of PSI and the non-photochemical energy dissipation due to the donor- and acceptor-side limitations (Klughammer and Schreiber 1994). Besides P700, Pcy also contributes to the light-induced absorbance change in the near infrared region dependent on its redox state (Harbinson and Hedley 1989; Klughammer and Schreiber 1991; Kirchhoff et al. 2004; Oja et al. 2003). Furthermore, changes in the redox state of Fd can be involved in the near infrared absorbance (Klughammer and Schreiber 1991). Recently, Klughammer and Schreiber have developed a new-type pulse-amplitude modulation spectrophotometer for the deconvolution of the signal of P700, Pcy, and Fd from the *in vivo* light-induced absorbance changes in near infrared regions (Schreiber and Klughammer 2016; Schreiber 2017; Klughammer and Schreiber 2016). The latest study by Sétif et al. (2019) has developed some methodological aspects of Klas-NIR spectrophotometer and determined the relative signal amplitudes of P700, Pcy, cyt c_6, Fd and (F_A F_B) *in vitro* using isolated PSI and its electron transport partners. Recent *in vivo* studies have mainly focused on the analyses of redox state and electron transport in Fd (Takagi and Miyake 2018; Kadota et al. 2019; Nikkanen et al. 2018; Vaseghi et al. 2018; Kumar et al. 2019). The present work is dedicated to the *in vivo* characterization of the luminal donors of PSI. First, for the extension of methodological aspects to *in vivo* Klas-NIR measurements, (1) the maximum P700 signals and initial photo-oxidation kinetics were compared between plant leaves and cyanobacterial suspensions, (2) cyt c_6 was detected in the cyanobacterium *T. elong.* and (3) the ratio of Pcy to P700 was quantified. Second, we chose one physiologically relevant condition, i.e. the start of leaf senescence, to demonstrate the pertinence of the Klas-NIR measurements for physiological studies. The quantities of the electron transport components around PSI can be significantly altered between the plant leaves at different ages (Krieger-Liszkay et al. 2019), and Pcy is one of the components that are lost from the photosynthetic electron transport system during the early stages of leaf senescence (Schöttler et al. 2004). The loss of Pcy and its consequence on electron donation to PSI were tested using Klas-NIR spectrophotometer, in parallel with other methods.

Materials and Methods

Plant and cyanobacterial materials

The winter barley cultivar Lomerit (*Hordeum vulgare* L., cv. Lomerit) was grown on soil in long-day laboratory growth condition (16 h-light, 70 µmol photons m^{-2} s^{-1}, white fluorescent lamp/8 h-dark). Primary leaves were used for all experiments before and after the onset of natural senescence.

The cyanobacterium *Synechocystis* sp. PCC 6803 (*S.* 6803) was grown in an incubator under continuous light (50 µmol photons m^{-2} s^{-1}) at 31°C. *T. elong.* was grown at 45°C under a light intensity of 70 µmol photons m^{-2} s^{-1}.

Determination of chlorophyll content

Chlorophyll was extracted from plant leaves by incubation for 1 day in the dark in 100% acetone. The contents of chlorophyll *a* and *b* were spectroscopically determined in 80% (v/v) acetone following the method of Arnon (1949).

The chlorophyll *a* content of cyanobacterial suspensions was spectroscopically determined using the extinction coefficient determined by Porra et al. (1989). The chlorophyll determination was made in parallel with the measurement of cell suspension absorption with a spectrophotometer minimizing the contribution of light-scattering (Kauny and Sétif 2014). From these parallel measurements, it was found that the chlorophyll content of a *S.* 6803 suspensions can be rather precisely estimated using an absorption coefficient of 64 ± 1.0 mM^{-1} cm^{-1} (average of 10 measurements) for the *in vivo* chlorophyll maximum at 679−680 nm (by reference to absorption at 750 nm). An identical coefficient was obtained by studying a *S.* 6803 mutant devoid of phycocyanin (gift of Dr. Ghada Ajlani), in accordance with the fact that the phycocyanin absorption is weak at the red chlorophyll maximum (Yamanaka et al. 1978). It should be noted that the above coefficient may lead to chlorophyll underestimation in cells having a large phycocyanin to chlorophyll ratio, since phycocyanin may significantly contribute to the absorption at 680 nm. In the present cases (*T. elong.* as well as *S.* 6803) where the ratio of the 625 nm to 680 nm absorption maxima is less than 1.1, this effect appears to be negligible.

Deconvolution of P700, Pcy, and Fd transmittance changes

The redox states of P700, Pcy and Fd were estimated from four original pulse-modulated dual-wavelength difference signals in the range of near-infrared (780–820, 820–870, 870–965 and 840–965 nm) using Klas-NIR spectrophotometer spectrophotometer (Walz, Effeltrich, Germany). For the deconvolution of P700, Pcy, and Fd transmittance changes in plant leaves, we determined the reference model spectra following the standard method previously described (Klughammer and Schreiber 2016). The measurements were made at the chlorophyll concentration of 8−15 µg mL^{-1} in the reaction cuvette. Whereas *S.* 6803 cells were measured in BG-11 medium, glycerol was added to *T. elong.* cells in BG-11 at 20% (v/v) just before the measurements in order to avoid cell sedimentation. Saturation pulse and actinic lights were provided by the LED array with a peak emission of 630 nm. Far-red light was provided by the LED array with a peak emission of 740 nm. The measurements were conducted using two different experimental settings of the software of Klas-NIR spectrophotometer, “Slow kinetics mode” for the data in Fig. 1, 2 and 4A, and “Fast kinetics mode” for those in Fig. 3A, 4C and 6.

Estimation of amplification factor

The maximum amplitude of the $P700^+$ signal measured with Klas-NIR spectrophotometer was compared to that expected from the chlorophyll content of a barley leaf section or a cyanobacterial suspension. After spectral deconvolution, the amplitudes of the different components, including $P700^+$, correspond to their respective contributions to the absorption changes at 902.5 nm and are given in units of $(\Delta I \times 10^{-3})/I$ in the software of Klas-NIR spectrophotometer (i.e. in units of $[\Delta A_{902.5} \times 2.3 \times 10^{-3}]$). Pseudo-coefficients of 4750, 3900 and 4750 M^{-1} cm^{-1} at 902.5 nm ($\varepsilon_{902.5}$) were previously measured for $P700^+$ of purified PSI respectively from tobacco, *S.* 6803 and *T. elong.* (Sétif et al. 2019). The pseudo-coefficient obtained from tobacco PSI was used for barley.

In plant leaves, the chlorophyll content was determined in number of moles of chlorophyll per cm^2 ($N_{chl/area}$) whereas the effective path length (L_{eff}; cm) is defined by Beer’s law:

$\Delta A_{902.5} = \varepsilon_{902.5\ nm} \times C_{PSI} \times L_{eff}$ (1)

where the PSI concentration (C_{PSI}) is obtained from $N_{chl/area}$:

$C_{PSI} = (N_{chl/area} \times S/V)/(N_{chl/P700})$ (2)

where $N_{chl/area}$, S, V and $N_{chl/P700}$ are the chlorophyll amount per leaf section (in mole/cm^2), the leaf section in cm^2, the leaf volume in dm^3 and the molar ratio of chlorophyll to P700 of thylakoid membranes assumed to be 380 in the plant leaves, respectively (Mullet et al. 1980).

One has: $V = S \times w \times 10^{-3}$ where S and the leaf thickness (w) are expressed in cm^2 and cm, so that:

$C_{PSI} = (N_{chl/area} \times 1000)/(w \times N_{chl/P700})$ (3)

Equation (1) can then be rewritten as follows.

$L_{eff}/w = (\Delta A_{902.5}/\varepsilon_{902.5}) \times (N_{chl/P700})/(N_{chl/area} \times 1000)$ (1')

The ratio of L_{eff} to w can be considered as an *in vivo* amplification factor corresponding to the fact that the effective pathlength is different from the leaf thickness. This factor is expected to be larger than 1 if *e.g.* the measuring light crosses several times the thylakoid membranes due to diffraction and scattering.

In cyanobacterial suspensions, C_{PSI} can be estimated from the chlorophyll *a* concentration (C_{chl}) with a cuvette optical path of 1 cm. The effective pathlength is also given by equation (1):

$L_{eff} = (\Delta A_{902.5}/\varepsilon_{902.5}) \times (N_{chl/P700})/C_{chl}$ (4)

In the present study, $N_{chl/P700}$ for cyanobacteria was assumed to be 108, which corresponds to a PSI/PSII ratio of 3 (counting a chlorophyll content of 96 and 36 for PSI and PSII, respectively). Thus, $N_{chl/P700}$ varies in a narrow range, from 114 to 102, when the PSI/PSII ratio varies from 2 to 6, a range which was currently estimated by electron paramagnetic resonance quantification in *S.* 6803 (Calzadilla et al. 2019) and *T. elong.* (Alain Boussac, personal communication).

Immunoblot analysis

Barley leaves were ground in a mortar in a buffer containing 100 mM HEPES-KOH (pH 7.5), 0.3 M sorbitol, 2 mM EDTA, 1 mM $MgCl_2$, and 0.25% (w/v) BSA, and the slurry was filtered through one layer of cheesecloths. For immunological detection, proteins of the extracts were separated by sodium dodecyl sulfate polyacrylamide gel electrophoresis (12%), and transferred onto a nitrocellulose membrane for immunodetection. Labelling of the membranes with antibodies was carried out at room temperature in 50 mM Tris-HCl (pH 7.6), 150 mM NaCl, 0.1% (v/v) Tween-20 and 4% non-fat milk powder. After washing, bound antibodies were revealed with a peroxidase-linked secondary anti-rabbit antibody and visualized by enhanced chemiluminescence. The polyclonal antibodies specific to Pcy (AS06 141), PsaE (AS08 324A), and cyt *f* (AS08 306), and the secondary antibodies were purchased from Agrisera (Vännäs, Sweden).

Results and Discussion

Responses of P700, Pcy and Fd to light are different in plants and cyanobacteria

The redox states of P700, Pcy and Fd were simultaneously analyzed using Klas-NIR spectrophotometer based on the reference model spectra determined in the intact barley leaves and the cyanobacterial suspensions of *S.* 6803 and *T. elong.* (Supplemental Fig. S1). The reference model spectra for each component were different among these organisms. Especially, the cells of *S.* 6803 used in this study showed a significantly higher transmittance difference around 850 nm

corresponding to P700, compared with barley and *T. elong.* (Supplemental Fig. S1), which indicates that the reference model spectra for P700 have a large variety in different species. Recently, the contributions of each component to Klas-NIR signals have been quantitatively estimated *in vitro* using isolated PSI, Pcy and Fd, resulting in approximately 20% and 2% as the ratio of the Pcy- and Fd-signal amplitudes to the P700-signal (Sétif et al. 2019). Reference model spectra for P700 obviously have a dominant impact on the deconvolution of all three components (Supplemental Fig. S1B), and special care has to be taken to determine its spectrum for each species studied.

In Fig. 1A, we show the responses of the redox states of P700, Pcy and Fd to red actinic and far-red light illumination in the primary leaves of young barley plants in the standard script "NIR Max" of the Klas-NIR spectrophotometer software. In darkness both P700 and Pcy are completely reduced, and Fd is expected to be fully oxidized. The maximum oxidation levels of P700 and Pcy are obtained by a saturation flash after far-red light illumination, and Fd is fully reduced by a saturation flash in actinic light illumination. As a result, "relative" values showing the amounts of total photo-oxidizable (or reducible) P700, Pcy and Fd were determined (Fig. 1A). These redox responses are typical for plant leaves as has been already reported (Schreiber 2017).

The cyanobacterial suspensions of *S.* 6803 showed kinetics of Klas-NIR signals different from those in plant leaves. In *S.* 6803, P700 becomes mostly oxidized at the end of a short illumination with actinic light and is kept more reduced under far-red light, compared with plants (Fig. 1B). These results are consistent with previous studies and are attributed to the electron transports from the acceptor side of PSI to O_2 mediated by flavodiiron protein and from the respiratory electron transport chain to PSI, both of which exist in cyanobacteria but not in angiosperms (Shimakawa et al. 2014; Shimakawa et al. 2019).

Here we analysed for the first time the redox states of Pcy and Fd simultaneously with P700 in cyanobacteria *in vivo*. The redox state of Pcy changes in parallel to that of P700 under actinic light whereas Pcy oxidation occurs prior to P700 oxidation in response to far-red light illumination (Fig. 1B). Different from plants, in cyanobacteria it should be noted that not only Pcy but also cyt c_6 function as the electron donor for PSI because many cyanobacterial species modulate the expression levels of Pcy and cyt c_6 dependent on the concentration of available copper in the medium. However, at least in a BG-11 medium (approximately 0.5 µM copper), *S.* 6803 mainly uses Pcy as the electron donor for PSI (Zhang et al. 1992).

In *S.* 6803, Fd is rapidly oxidized during the actinic light illumination, compared with barley leaves. In parallel P700 is oxidized (Fig. 1B). The difference in the redox state of Fd can be attributed to the function of flavodiiron protein. One can note that the Fd signal during the actinic light illumination may contain a contribution from (F_A F_B) as Fd and (F_A F_B) give similar Klas-NIR signals (Sétif et al. 2019). Further studies of Fd in cyanobacteria deserve a detailed investigation and are outside the scope of the present study. Hereafter, we often show the Klas-NIR signals of P700, Pcy and Fd as the redox state (%) to the maximum oxidation (reduction) amplitudes.

The Klas-NIR signals are largely amplified in plant leaves but not in cyanobacterial suspensions

In the present study, the maximum amplitude of the $P700^+$ signal given by the Klas-NIR spectrophotometer was compared to that expected from the chlorophyll content of a barley leaf section or a cyanobacterial suspension (see "Materials and Methods"). The "expected" signal was calculated by using the $P700^+$ absorption coefficient determined *in vitro* (Sétif et al. 2019) and by assuming that transmittance follows regular Beer's law, with C × w (concentration × pathlength) being the product of $P700^+$ concentration (determined from the Chl/P700 ratio) and the leaf thickness or the width of the cuvette containing cyanobacteria. This implicitly assumes that the NIR measuring light goes straightforward from the emitter to the detector and is absorbed only once by each $P700^+$. We found that the Klas-NIR $P700^+$ amplitude is significantly higher than the expected one in plant

leaves but not in cyanobacterial suspensions (Table 1). Thus Beers's law is approx. valid in cyanobacterial suspensions but is not for leaves and an effective pathlength L_{eff} should therefore be considered. The ratio of L_{eff} to the leaf thickness, termed as "amplification factor", is approximately 6.5 and 5 in barley and spinach leaves, respectively (Table 1). In the case of cyanobacterial suspensions, the amplification factor was defined as the ratio of L_{eff} to the cuvette width, which gave values close to 1 both in *S.* 6803 and *T. elong.* (Table 1). These data suggest that the near infrared measuring beams undergo multiple reflections inside the plant leaves, which results in larger signals of P700, Pcy and Fd than those in cyanobacterial suspensions. An infiltration of spinach leaves with water lowered the amplification factor to about a half (Table 1). Additionally, the values were the same in leaves infiltrated with 0.2 M sucrose. This indicates that the 50% decrease in amplification factor was not related to changes of cell structure by osmotic pressure and that the intercellular space filled with air has the main impact on light reflections. A slightly higher amplification factor was observed in *T. elong.* than in *S.* 6803 (Table 1). *T. elong.*cells are rods while *S.* 6803 cells are spherical, and the rod shape possibly increases light reflection and amplification factor.

Cyt c_6 is observable *in vivo* with Klas-NIR spectrophotometer in *T. elong.*

In vitro experiments have shown that the soluble electron carrier cyt c_6 can also be analysed by Klas-NIR spectrophotometer because of its absorbance in near infrared regions (Sétif et al. 2019). In the following, we investigated *in vivo* the light-induced changes in the redox state of cyt c_6 using the cyanobacterium *T. elong.*, which utilizes only cyt c_6 as the electron donor for PSI. For the measurements, the reference model spectrum for P700 in *T. elong.* was newly determined *in vivo* (Supplemental Fig. S1), and we used the reference model spectra for cyt c_6 and Fd determined using purified proteins *in vitro* (Sétif et al. 2019). The responses of P700, cyt c_6 and Fd to an actinic light were analysed with or without 3-(3,4-dichlorophenyl)-1,1-dimethylurea (DCMU) and methyl viologen (MV). In response to the illumination with a saturation flash, P700 was kept oxidized, paralleled by the oxidation of cyt c_6. Simultaneously with the induction of P700 and cyt c_6 oxidation at 0.5 s, Fd started to be oxidized (Fig. 2A). These results are similar to those of P700, Pcy and Fd in *S.* 6803 (Fig. 1B) and might be related to the function of flavodiiron protein. In the presence of DCMU and MV, expectedly, both P700 and cyt c_6 were kept oxidized during the illumination with an actinic light, and no Fd reduction was observable (Fig. 2B). Further, the reduction of P700 and cyt c_6 was largely slowed down in the presence of DCMU and MV. From these facts, we concluded that the redox state of cyt c_6 can be analysed *in vivo* in *T. elong.* despite of the smaller signal size than that of Pcy. Notably, a false deconvolution of these data with the reference model spectrum for Pcy instead of that for cyt c_6 gave no positive Pcy signal (data not shown). This supports the present deconvolution involving cyt c_6. We note that cyt *f* of cyt b_6f complex also harbours a *c*-type heme and possibly contributes to the cyt c_6 signal. However, the contribution of cyt *f* to the near infrared absorbance has not yet been experimentally shown, and therefore we cannot conclude at the present stage on cyt *f* contribution to Klas-NIR signals.

The ratio of Pcy to P700 can be quantified with Klas-NIR spectrophotometer

As shown in Fig. 1, Klas-NIR spectrophotometer gives relative values for $P700^+$, Pcy^+ and Fd^-. This present study sought to quantify the ratio of Pcy to P700 *in vivo*. For the determination of the "absolute ratio" of Pcy to PSI, the electron transport between Pcy and P700 was analyzed in short-saturation flashes repetitively applied three times with 1 ms intervals. In the case of PSI, even a 5 µs short-saturation flash can cause some double turnover because of a fast electron donation from PSI-bounded Pcy to $P700^+$ with a 11 µs half time (Drepper et al. 1996). Additionally, the electron transport from cyt *f* to Pcy^+ is also fast (the half time is 35−350 µs) (Hope 2000), whereas the reduction of cyt *f* in the cyt b_6f complex is relatively slow (10−20 ms) and known as a limiting step of

photosynthetic electron transport system (Chow and Hope 2004; Stiehl and Witt 1969). Compared with the rapid $P700^+$ reduction by Pcy, the reduction of Pcy^+ after the short-saturation flash was very slow (Fig. 3A). Further, just after the first flash, Pcy was kept oxidized at an almost constant level whereas $P700^+$ was undergoing some reduction (Fig. 3A), which suggests that in this phase Pcy^+ formed via reduction of $P700^+$ was simultaneously reduced by cyt *f*. Finally, after the third flash Pcy was further oxidized in parallel with the reduction of $P700^+$ (Fig. 3A), which can simply reflect the electron transport from Pcy to $P700^+$ if we assume that cyt *f* is almost completely oxidized during this phase. Based on these assumptions, the molar ratio of Pcy to P700 was determined as the slope of the correlation of $P700^+$ with Pcy^+ (2.53 ± 0.25, n = 3; Fig. 3B and Table 2), which was within the range of the Pcy quantity reported by previous studies using *in vitro* assays (Plesniçar and Bendall 1970; Katoh et al. 1961; Burkey 1993; Oja et al. 2003). One concern is that cyt f^+ is possibly back-reduced by Pcy by redox equilibration because of the small difference in midpoint potentials of the 2 species (Sacksteder and Kramer 2000). This would result in an underestimation of the Pcy/P700 ratio, but it is unlikely to occur when Pcy is highly oxidized (Fig. 3A).

There are several other ways to quantify the ratio of Pcy to P700 (i.e. PSI) *in vivo* with Klas-NIR spectrophotometer. For example, if we assume that the absorption coefficients of P700 and Pcy determined *in vitro* (Sétif et al. 2019) are also valid *in vivo*, the molar ratio of Pcy to P700 should be:

$$Pcy/P700 = Pcy_{max}/(P700_{max} \times 0.21) \quad (5)$$

The values of Pcy_{max} and $P700_{max}$ correspond to the maximum oxidation amplitudes of these components as shown in Fig. 1. The value 0.21 reflects the contribution of Pcy to the Klas-NIR signal as compared with P700, determined *in vitro* (Sétif et al. 2019). From this calculation, the Pcy/P700 ratio was estimated 4.4 ± 0.4 (n = 3) in the primary leaves of barley, which is significantly larger than that estimated in Fig. 3B. In equation 5 we assume that the amplification factor between Pcy and P700 is the same. The discrepancy between the ratio of Pcy to P700 determined in Fig. 3 and by equation 5 may be caused by a difference in the amplification factor of P700 and Pcy or, as mentioned above, by a possible electron transport from Pcy back to cyt f^+.

Loss of Pcy was detected *in vivo* in senescing barley leaves with Klas-NIR spectrophotometer

Here we sought to demonstrate the relevance of the Klas-NIR measurements for physiological studies by following absorption changes during leaf senescence. It has been known that the photosynthetic electron transport system is altered during leaf senescence, and that some of these alterations are earlier than the loss of chlorophyll, a popular marker of leaf senescence (Krieger-Liszkay et al. 2019). For example, the cyt b_6f complex shows a rapid loss upon leaf senescence (Ben-David et al. 1983). Pcy is also one of the components that is lost at an early stage of leaf senescence (Schöttler et al. 2004). The loss of Pcy can therefore be a useful marker for the initiation of leaf senescence in plant leaves, and the Klas-NIR measurements are expected to be practical to quickly and non-invasively check the status of leaf senescence.

In Fig. 4A, we show the responses of the redox states of P700, Pcy and Fd in the standard script “NIR Max” in the primary leaves of barley 17 days after sowing. Compared with the leaves of younger plants (10 days after sowing; Fig. 1A), P700 and Pcy components were more oxidized during the illumination with an actinic light (Fig. 4A). Additionally, the amplitude of maximum Pcy oxidation was significantly smaller in the 17 days plants than in the 10 days old plants, by reference to the maximum $P700^+$ amplitude. From such data on primary leaves, we evaluated the relative Pcy to P700 ratio at different growth stages of the same plant species, which is calculated from the relative transmittance values in Klas-NIR signals for $P700^+$ and Pcy^+, in parallel with chlorophyll measurements. As shown in Fig. 4B, the content of Pcy obviously decreased earlier than that of chlorophyll during barley senescence. Further, the absolute Pcy to P700 ratio was quantified according to the method shown in Fig. 3 using the primary leaves of barley 17 days after sowing (Fig. 4C and D), giving a molar ratio of

1.58 ± 0.19 (*n* = 3; Fig. 4D and Table 2). However, from the calculation using the equation (5), the Pcy/P700 molar ratio was estimated 3.2 ± 0.2 (*n* = 3) in the 17 days old leaves.

The early decrease in Pcy during leaf senescence was shown also by immunoblotting using specific antibodies. The amount of Pcy clearly decreased in the primary leaves from 10 to 17 days after sowing (Fig. 5) whereas those of PsaE (a PSI subunit) and cyt *f* remained constant. These data are in agreement with the results of the Klas-NIR measurement, and suggest that the loss of Pcy is even earlier than that of cyt *f* at the early stage of leaf senescence.

To evaluate the effect of the loss of Pcy at the early stage of senescence on photosynthetic electron transport, we measured the kinetics of re-reduction of $P700^+$ and Pcy^+ in the transition from light to dark at steady-state photosynthesis in the primary leaves of barley. The leaves were illuminated with an actinic light for 15 min, giving stable values of P700, Pcy and Fd signals, then the actinic light was turned off. Whereas both $P700^+$ and Pcy^+ immediately started to be reduced in the transition from light to dark in the leaves of 10 days old plants, in 17 days old ones the reduction of Pcy^+ was delayed and showed a sigmoidal kinetics with a lag phase in the reduction of Pcy^+ (Fig. 6). After the lag phase the decay of Pcy^+ was similar to that in the 10 days old plants (Fig. 6A). These data indicate that the reduction of Pcy^+ by the cyt b_6f complex was slowed down in early senescing leaves, compared with mature leaves. It has already been reported previously that the decrease in the amount of Pcy limits electron transport on the donor side of PSI using isolated thylakoid membranes (Schöttler et al. 2004), probably due to the limitation of the lateral diffusion of Pcy between the cyt b_6f complex and PSI (Drepper et al. 1996; Haehnel 1982; Cruz et al. 2001). In our study, we demonstrated the retarded re-reduction of Pcy^+ *in vivo* using intact leaves. A slow diffusion of Pcy between the cyt b_6f complex and PSI does not matter when the pool of Pcy relative to PSI is large, but it becomes crucial when the amount of Pcy decreases, finally limiting photosynthetic linear electron transport.

Acknowledgements

The authors most gratefully thank Dr. Christof Klughammer for his help in installing Klas-NIR spectrophotometer and in using the associated software. Dr. Klughammer also pointed to us the apparent amplification of the $P700^+$ signal in leaves. This work benefits from the support of the LabEx Saclay Plant Sciences-SPS (ANR-10-LABX-0040-SPS) and the French Infrastructure for Integrated Structural Biology (FRISBI) ANR-10-INSB-05, and also partially supported by a grant from the Agence Nationale de la Recherche (RECYFUEL project ANR-16-CE05-0026). The authors also thank Dr. Karin Krupinska (University of Kiel, Germany) for giving the barley seeds, Dr. Cristian Ilioaia (I2BC) for culturing spinach, Dr. Alain Boussac (I2BC) for cultures of *T. elong.*, and Dr. Diana Kirilovsky (I2BC) for her help in culturing *S.* 6803. G.S. is supported by a JSPS oversea research fellowship (201860126).

Tables

Table 1. Amplification factor in plant leaves and cyanobacterial suspensions

Barley (10 days)	6.7 ± 0.4
Barley (17 days)	6.5 ± 0.3
Spinach (intact)	5.1 ± 0.7
Spinach (H_2O-infiltrated)	2.7 ± 0.3
Spinach (0.2 M sucrose-infiltrated)	3.0 ± 0.5
S. 6803	1.06 ± 0.05
T. elongatus	1.38 ± 0.04

Data are shown in the mean with standard deviation (biological replicates; *n* = 3 (plant material) or 4 (cyanobacterial cultures).

Table 2. Absolute ratio of plastocyanin to photosystem I (P700) in barley leaves

	10 days after sowing	17 days after sowing
Barley leaves	2.53 ± 0.25	1.58 ± 0.19

Data are shown in the mean with standard deviation (three biological replicates).

Figure legends

Fig. 1. Changes of the redox states of P700 (green), plastocyanin (Pcy; blue) and ferredoxin (Fd; wine red) to illuminations with red actinic light (930 µmol photons m^{-2} s^{-1}, 3−6 s) and far-red light (10−20 s) in primary leaves of barley 10 days after sowing (A) and in the cyanobacterial suspensions of *Synechocystis* sp. PCC 6803 (B). Saturation flashes (30 and 200 ms, respectively) were applied at 4 and 20 s as indicated by triangles. Fd^- is presented in negative values. Typical traces are shown.

Fig. 2. Responses of the redox states of P700 (green), cytochrome (cyt) c_6 (pink) and ferredoxin (Fd; wine red) to illuminations with actinic light in cyanobacterial suspensions of *T. elong*. (A) Cells were illuminated with a saturation flash for 1 s. (B) Cells were illuminated with red actinic light (600 µmol photons m^{-2} s^{-1}) for 2 s in the presence of 250 µM MV and 20 µM DCMU. Cyt c_6^+ and Fd^- are presented in negative values. Typical traces are shown.

Fig. 3. Quantitative evaluation of the ratio of plastocyanin (Pcy) to P700 in primary leaves of barley 10 days after sowing. (A) Responses of the redox states of P700 (green) and Pcy (blue) to 5-µs saturation flashes repetitively applied three times at 0, 1 and 2 ms as indicated by triangles. The 100% values correspond to the maximum oxidation amplitudes of P700 and Pcy. A typical trace is shown. (B) Correlation between $P700^+$ and Pcy^+ from 2.2 to 2.9 ms in Fig. 3A. Red line: linear regression (R^2 = 0.8014).

Fig. 4. Loss of plastocyanin (Pcy) in primary leaves of barley 17 days after sowing measured by Klas-NIR spectrophotometer. (A) Responses of the redox states of P700 (green), Pcy (blue) and ferredoxin (Fd; wine red) to illuminations with a red actinic light and a far-red light. Details of the script are described in Fig. 1. (B) The time courses of the relative ratio of Pcy to P700 (closed circles) and total chlorophyll content (open triangles) in primary leaves of barley. Data are shown as the mean with standard deviation of three biological replicates. (C) Responses of the redox states of P700 (green) and Pcy (blue) to 5-µs saturation flashes repetitively applied three times at 0, 1, and 2 ms as indicated by triangles. The 100% values correspond to the maximum oxidation amplitudes of P700 and Pcy. (D) Correlation between $P700^+$ and Pcy^+ from 2.2 to 2.9 ms in Fig. 4A. Dashed red line: linear regression (R^2 = 0.7900).

Fig. 5. Immunologically-detected plastocyanin (Pcy), PsaE subunit of PSI, and cytochrome (cyt) *f* by specific antibodies in the primary leaves of barley.

Fig. 6. Kinetics of re-reduction of oxidized plastocyanin (Pcy^+; A) and $P700^+$ (B) in the transition from light to dark at the steady-state photosynthesis in the primary leaves of barley 10 (darker colors) and 17 days (lighter colors) after sowing. Red actinic light (930 µmol photons m^{-2} s^{-1}) was turned off at the time zero. The 100% values correspond to the maximum oxidation amplitudes of P700 and Pcy.

Supplemental Fig. S1. Reference model spectra in barley (closed symbols, solid lines) and *Synechocystis* sp. PCC 6803 (open symbols, dashed lines) for P700 (green circles), plastocyanin (Pcy; blue diamonds) and ferredoxin (Fd; wine red triangles). The model spectrum for P700 in *Thermosynechococcus elongatus* is shown in blue crosses (dotted line). The mean values of the transmittance differences of four wavelength pairs are shown in the central wavelength respectively.

The spectra are normalized at 902.5 nm (A) and re-plotted in according to the contributions of each component to the Klas-NIR signals reported by Sétif et al. (2019) (B).

References

Arnon DI (1949) Copper enzymes in isolated chloroplasts. Polyphenoloxidase in *Beta vulgaris*. Plant Physiol 24:1-15

Ben-David H, Nelson N, Gepstein S (1983) Differential changes in the amount of protein complexes in the chloroplast membrane during senescence of oat and bean leaves. Plant Physiol 73:507-510

Burkey KO (1993) Effect of growth irradiance on plastocyanin levels in barley. Photosynth Res 36:103-110

Calzadilla PI, Zhan J, Sétif P, Lemaire C, Solymosi D, Battchikova N, Wang Q, Kirilovsky D (2019) The cytochrome b_6f complex is not involved in cyanobacterial state transitions. Plant Cell 31:911-931

Chow WS, Hope AB (2004) Kinetics of reactions around the cytochrome *bf* complex studied in intact leaf disks. Photosynth Res 81:153-163

Cruz JA, Salbilla BA, Kanazawa A, Kramer DM (2001) Inhibition of plastocyanin to P_{700}^+ electron transfer in *Chlamydomonas reinhardtii* by hyperosmotic stress. Plant Physiol 127:1167-1179

Drepper F, Hippler M, Nitschke W, Haehnel W (1996) Binding dynamics and electron transfer between plastocyanin and photosystem I. Biochemistry 35:1282-1295

Haehnel W (1982) On the functional organization of electron transport from plastoquinone to Photosystem I. Biochim Biophys Acta Bioenerg 682:245-257

Harbinson J, Hedley CL (1989) The kinetics of P-700$^+$ reduction in leaves: a novel in situ probe of thylakoid functioning. Plant Cell Environ 12:357-369

Harbinson J, Woodward FI (1987) The use of light-induced absorbance changes at 820 nm to monitor the oxidation state of P-700 in leaves. Plant Cell Environ 10:131-140

Hope AB (2000) Electron transfers amongst cytochrome *f*, plastocyanin and photosystem I: kinetics and mechanisms. Biochim Biophys Acta Bioenerg 1456:5-26

Kadota K, Furutani R, Makino A, Suzuki Y, Wada S, Miyake C (2019) Oxidation of P700 induces alternative electron flow in photosystem I in wheat leaves. Plants 8:152

Katoh S, Suga I, Shiratori I, Takamiya A (1961) Distribution of plastocyanin in plants, with special reference to its localization in chloroplasts. Arch Biochem Biophys 94:136-141

Kauny J, Sétif P (2014) NADPH fluorescence in the cyanobacterium *Synechocystis* sp. PCC 6803: A versatile probe for in vivo measurements of rates, yields and pools. Biochim Biophys Acta Bioenerg 1837:792-801

Kirchhoff H, Schöttler MA, Maurer J, Weis E (2004) Plastocyanin redox kinetics in spinach chloroplasts: evidence for disequilibrium in the high potential chain. Biochim Biophys Acta Bioenerg 1659:63-72

Klughammer C, Schreiber U (1991) Analysis of light-induced absorbance changes in the near-infrared spectral region I. Characterization of various components in isolated chloroplasts. Zeitschrift für Naturforschung C, vol 46.

Klughammer C, Schreiber U (1994) An improved method, using saturating light pulses, for the determination of photosystem I quantum yield via P700$^+$-absorbance changes at 830 nm. Planta 192:261-268

Klughammer C, Schreiber U (2016) Deconvolution of ferredoxin, plastocyanin, and P700 transmittance changes in intact leaves with a new type of kinetic LED array spectrophotometer. Photosynth Res 128:195-214

Krieger-Liszkay A, Krupinska K, Shimakawa G (2019) The impact of photosynthesis on initiation of leaf senescence. Physiol Plant 166:148-164

Kumar V, Vogelsang L, Seidel T, Schmidt R, Weber M, Reichelt M, Meyer A, Clemens S, Sharma SS, Dietz K-J (2019) Interference between arsenic-induced toxicity and hypoxia. Plant Cell Environ 42:574-590

Mullet JE, Burke JJ, Arntzen CJ (1980) Chlorophyll proteins of photosystem I. Plant Physiol 65:814-822

Nikkanen L, Toivola J, Trotta A, Diaz MG, Tikkanen M, Aro E-M, Rintamäki E (2018) Regulation of cyclic

electron flow by chloroplast NADPH-dependent thioredoxin system. Plant Direct 2:e00093
Oja V, Eichelmann H, Peterson RB, Rasulov B, Laisk A (2003) Deciphering the 820 nm signal: redox state of donor side and quantum yield of Photosystem I in leaves. Photosynth Res 78:1
Plesniçar M, Bendall DS (1970) The plastocyanin content of chloroplasts from some higher plants estimated by a sensitive enzymatic assay. Biochim Biophys Acta Bioenerg 216:192-199
Porra R, Thompson W, Kriedelman P (1989) Determination of accurate extraction and simultaneously equation for assaying chlorophyll a and b extracted with different solvents: verification of the concentration of chlorophyll standards by atomic absorption spectroscopy. Biochim Biophys Acta 975:384-394
Sétif P, Boussac A, Krieger-Liszkay A (2019) Near infrared *in vitro* measurements of photosystem I cofactors and electron-transfer partners with a recently-developed spectrophotometer. Photosynth Res In press
Sacksteder CA, Kramer DM (2000) Dark-interval relaxation kinetics (DIRK) of absorbance changes as a quantitative probe of steady-state electron transfer. Photosynth Res 66:145-158
Schöttler MA, Kirchhoff H, Weis E (2004) The role of plastocyanin in the adjustment of the photosynthetic electron transport to the carbon metabolism in tobacco. Plant Physiol 136:4265-4274
Schreiber U (2017) Redox changes of ferredoxin, P700, and plastocyanin measured simultaneously in intact leaves. Photosynth Res:1-18
Schreiber U, Klughammer C (2016) Analysis of photosystem I donor and acceptor sides with a new type of online-deconvoluting kinetic LED-array spectrophotometer. Plant Cell Physiol 57:1454-1467
Schreiber U, Klughammer C, Neubauer C (1988) Measuring P700 absorbance changes around 830 nm with a new type of pulse modulation system. Zeitschrift für Naturforschung C, vol 43.
Shimakawa G, Hasunuma T, Kondo A, Matsuda M, Makino A, Miyake C (2014) Respiration accumulates Calvin cycle intermediates for the rapid start of photosynthesis in *Synechocystis* sp. PCC 6803. Biosci Biotechnol Biochem 78:1997-2007
Shimakawa G, Murakami A, Niwa K, Matsuda Y, Wada A, Miyake C (2019) Comparative analysis of strategies to prepare electron sinks in aquatic photoautotrophs. Photosynth Res 139:401-411
Stiehl HH, Witt HT (1969) Quantitative treatment of the function of plastoquinone in photosynthesis. Zeitschrift für Naturforschung B, vol 24.
Takagi D, Miyake C (2018) PROTON GRADIENT REGULATION 5 supports linear electron flow to oxidize photosystem I. Physiol Plant 164:337-348
Vaseghi M-J, Chibani K, Telman W, Liebthal MF, Gerken M, Schnitzer H, Mueller SM, Dietz K-J (2018) The chloroplast 2-cysteine peroxiredoxin functions as thioredoxin oxidase in redox regulation of chloroplast metabolism. eLife 7:e38194
Yamanaka G, Glazer AN, Williams RC (1978) Cyanobacterial phycobilisomes. Characterization of the phycobilisomes of *Synechococcus* sp. 6301. J Biol Chem 253:8303-8310
Zhang L, McSpadden B, Pakrasi HB, Whitmarsh J (1992) Copper-mediated regulation of cytochrome c_{553} and plastocyanin in the cyanobacterium *Synechocystis* 6803. J Biol Chem 267:19054-19059

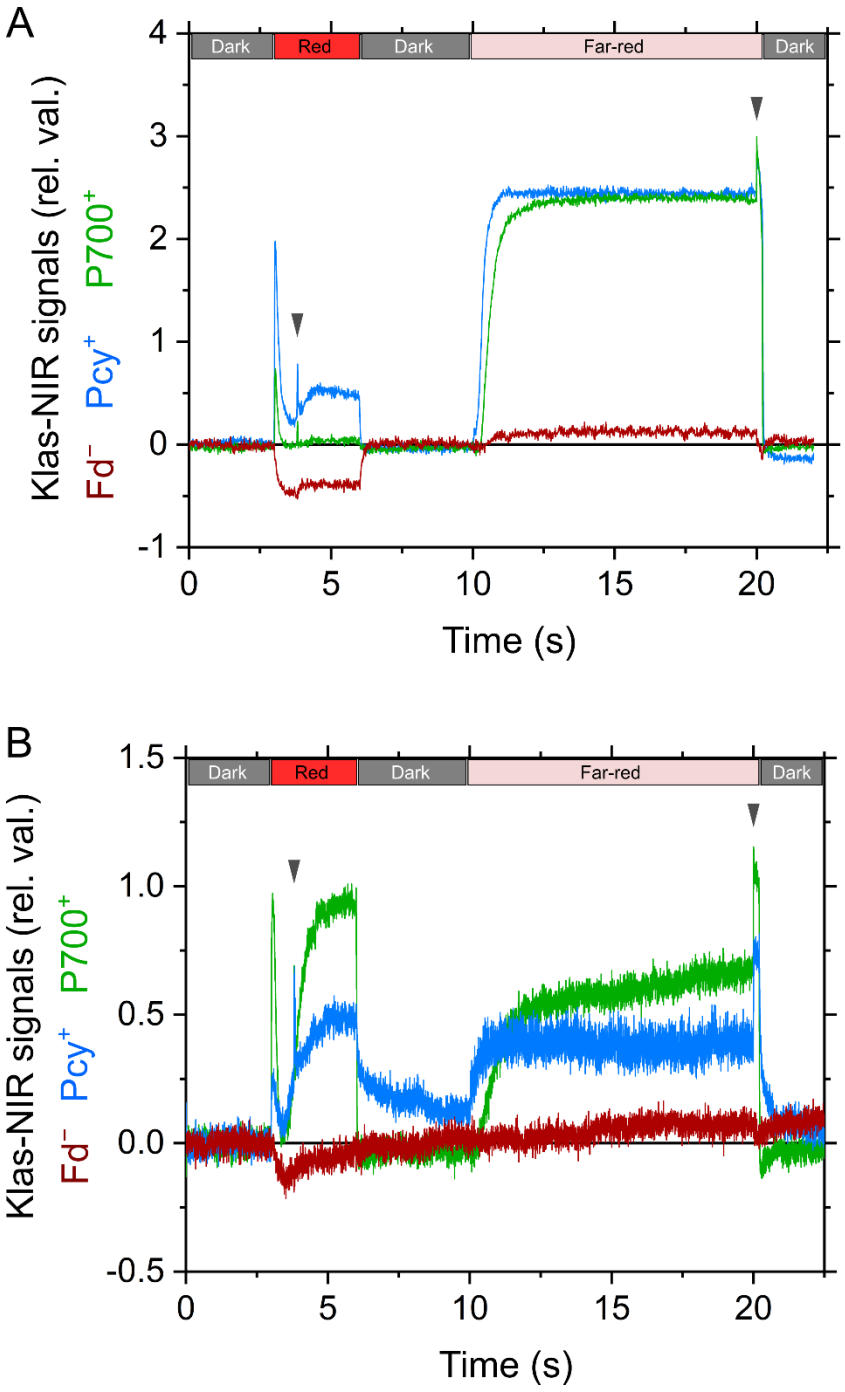

Fig. 1. Changes of the redox states of P700 (green), plastocyanin (Pcy; blue) and ferredoxin (Fd; wine red) to illuminations with red actinic light (930 µmol photons m^{-2} s^{-1}, 3–6 s) and far-red light (10–20 s) in primary leaves of barley 10 days after sowing (A) and in the cyanobacterial suspensions of *Synechocystis* sp. PCC 6803 (B). Saturation flashes (30 and 200 ms, respectively) were applied at 4 and 20 s as indicated by triangles. Fd^- is presented in negative values. Typical traces are shown.

Figure 1. Shimakawa et al.

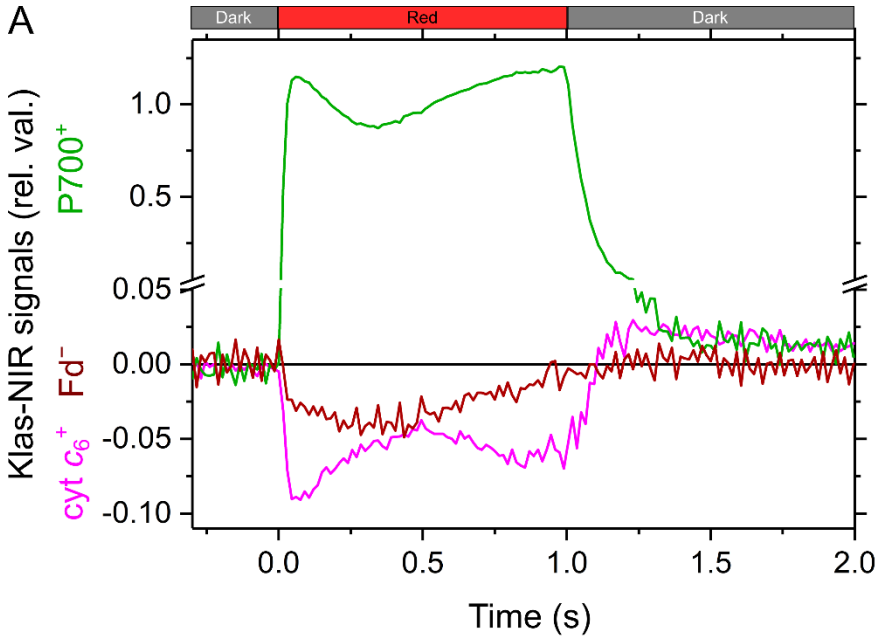

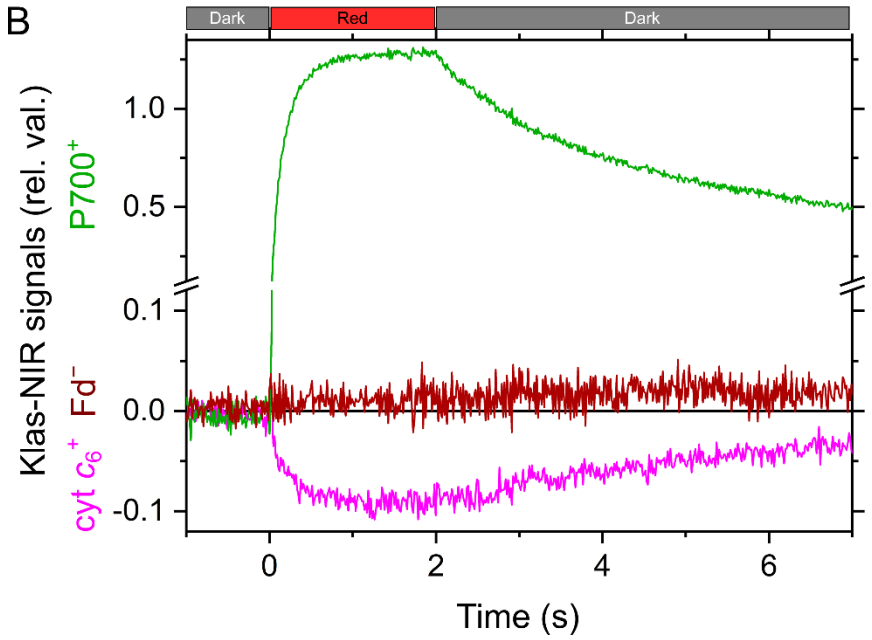

Fig. 2. Responses of the redox states of P700 (green), cytochrome (cyt) c_6 (pink) and ferredoxin (Fd; wine red) to illuminations with actinic light in cyanobacterial suspensions of *T. elong*. (A) Cells were illuminated with a saturation flash for 1 s. (B) Cells were illuminated with red actinic light (600 µmol photons m^{-2} s^{-1}) for 2 s in the presence of 250 µM MV and 20 µM DCMU. Cyt c_6^+ and Fd^- are presented in negative values. Typical traces are shown.

Figure 2. Shimakawa et al.

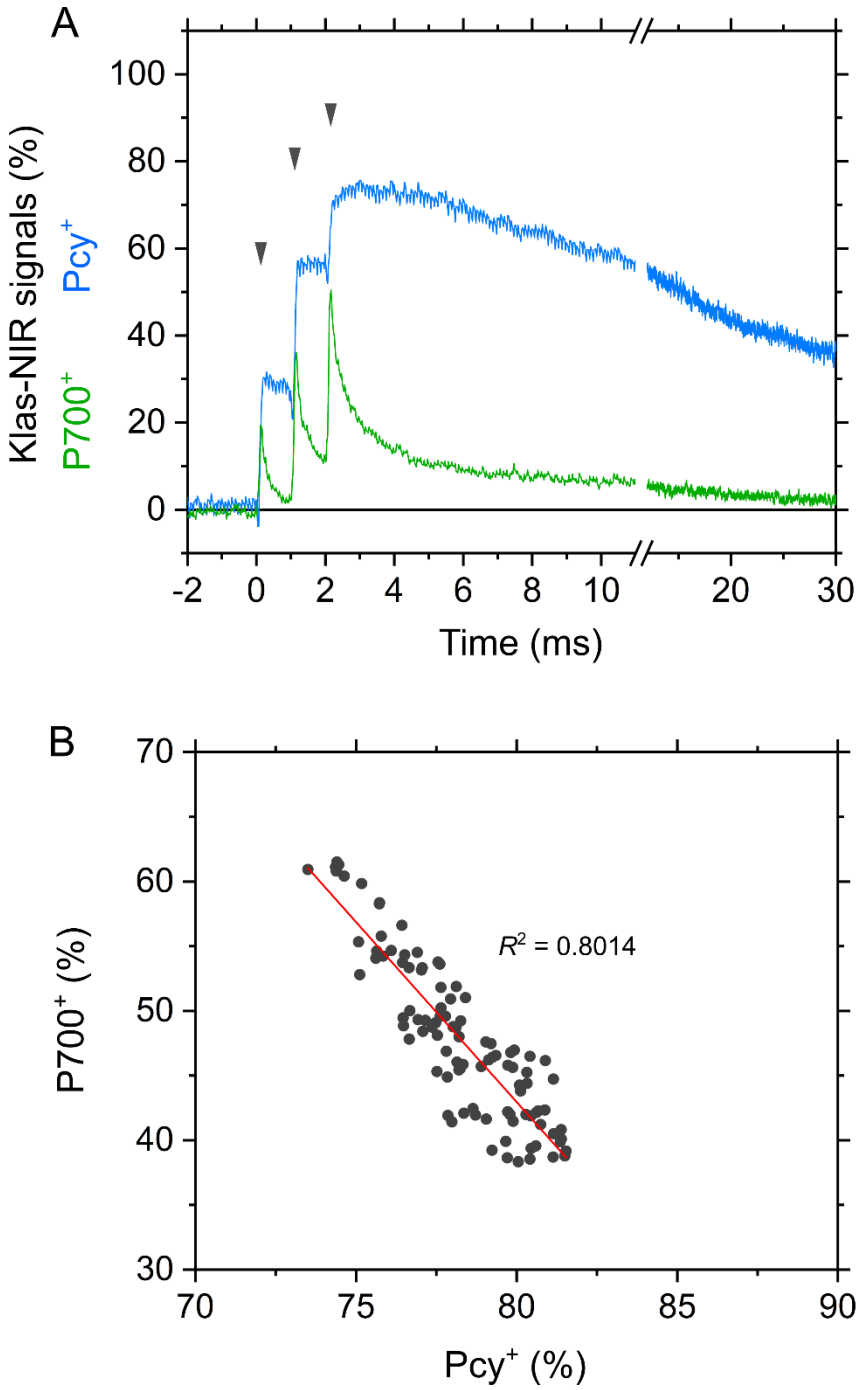

Fig. 3. Quantitative evaluation of the ratio of plastocyanin (Pcy) to P700 in primary leaves of barley 10 days after sowing. (A) Responses of the redox states of P700 (green) and Pcy (blue) to 5-µs saturation flashes repetitively applied three times at 0, 1 and 2 ms as indicated by triangles. The 100% values correspond to the maximum oxidation amplitudes of P700 and Pcy. A typical trace is shown. (B) Correlation between $P700^+$ and Pcy^+ from 2.2 to 2.9 ms in Fig. 3A. Red line: linear regression (R^2 = 0.8014).

Figure 3. Shimakawa et al.

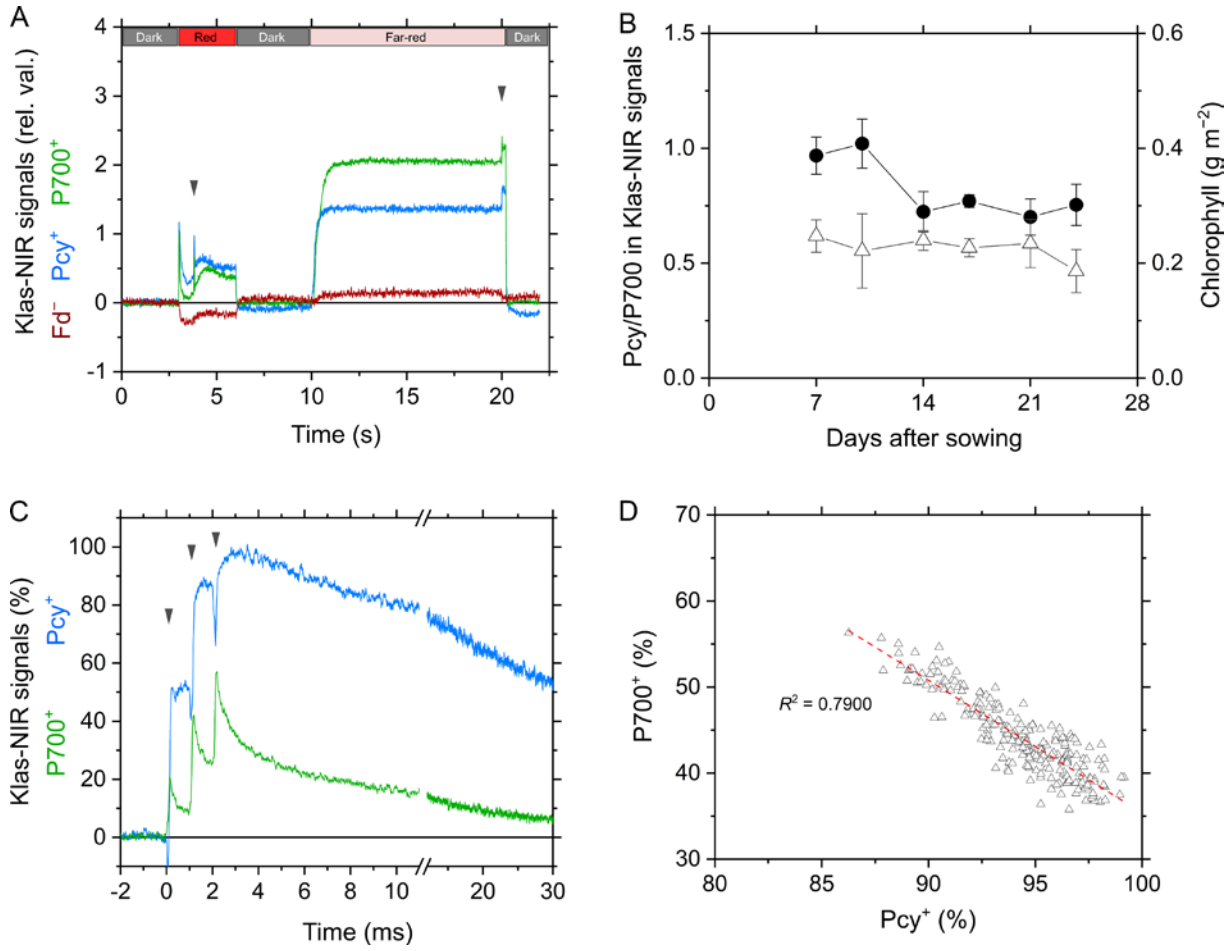

Fig. 4. Loss of plastocyanin (Pcy) in primary leaves of barley 17 days after sowing measured by Klas-NIR spectrophotometer. (A) Responses of the redox states of P700 (green), Pcy (blue) and ferredoxin (Fd; wine red) to illuminations with a red actinic light and a far-red light. Details of the script are described in Fig. 1. (B) The time courses of the relative ratio of Pcy to P700 (closed circles) and total chlorophyll content (open triangles) in primary leaves of barley. Data are shown as the mean with standard deviation of three biological replicates. (C) Responses of the redox states of P700 (green) and Pcy (blue) to 5-µs saturation flashes repetitively applied three times at 0, 1, and 2 ms as indicated by triangles. The 100% values correspond to the maximum oxidation amplitudes of P700 and Pcy. (D) Correlation between $P700^+$ and Pcy^+ from 2.2 to 2.9 ms in Fig. 4A. Dashed red line: linear regression (R^2 = 0.7900).

Figure 4. Shimakawa et al.

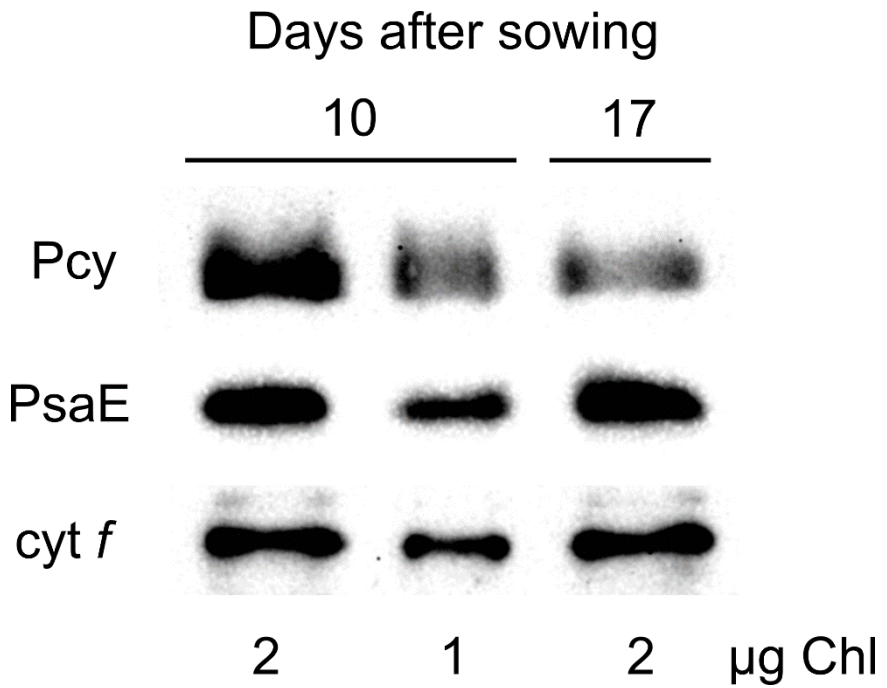

Fig. 5. Immunologically-detected plastocyanin (Pcy), PsaE subunit of PSI, and cytochrome (cyt) *f* by specific antibodies in the primary leaves of barley.

Figure 5. Shimakawa et al.

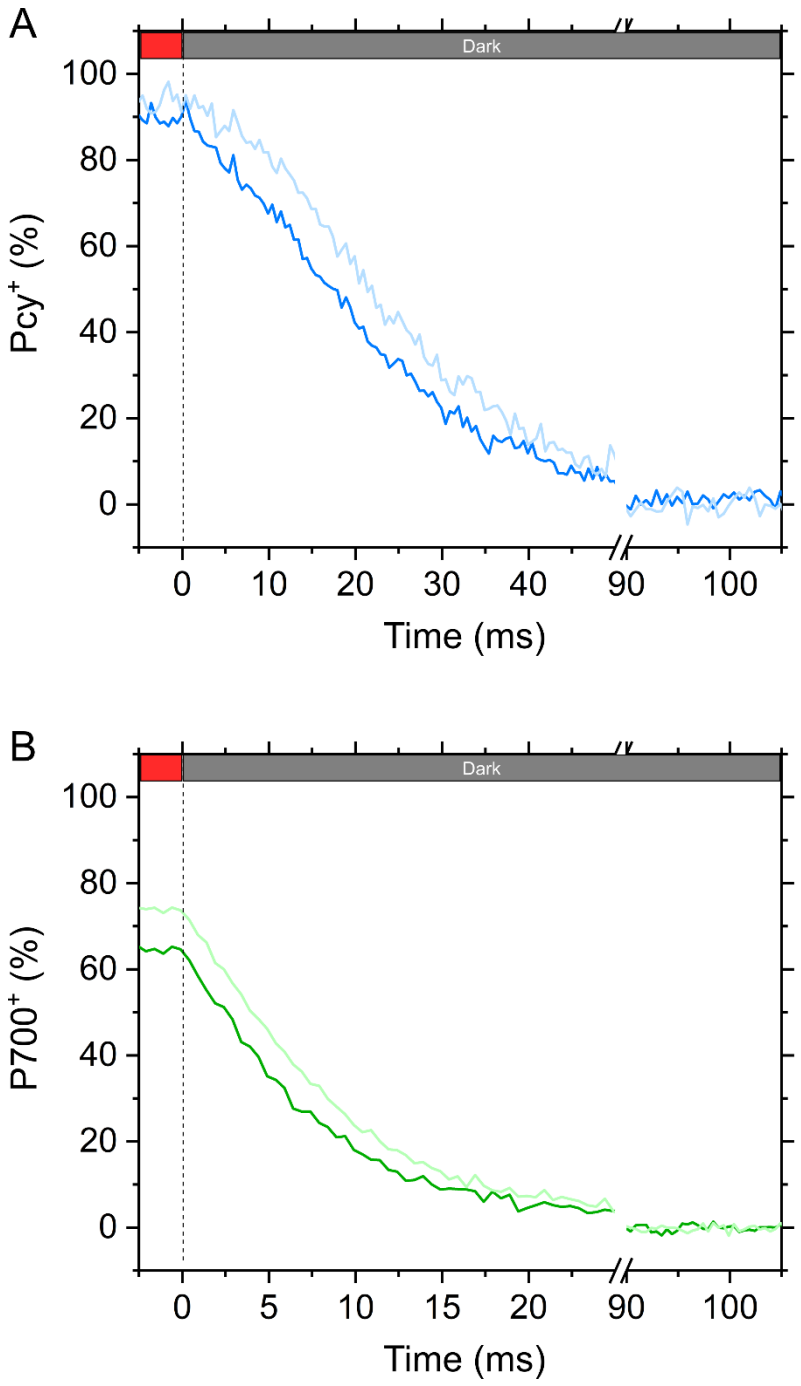

Fig. 6. Kinetics of re-reduction of oxidized plastocyanin (Pcy^+; A) and $P700^+$ (B) in the transition from light to dark at the steady-state photosynthesis in the primary leaves of barley 10 (darker colors) and 17 days (lighter colors) after sowing. Red actinic light (930 µmol photons m^{-2} s^{-1}) was turned off at the time zero. The 100% values correspond to the maximum oxidation amplitudes of P700 and Pcy.

Figure 6. Shimakawa et al.

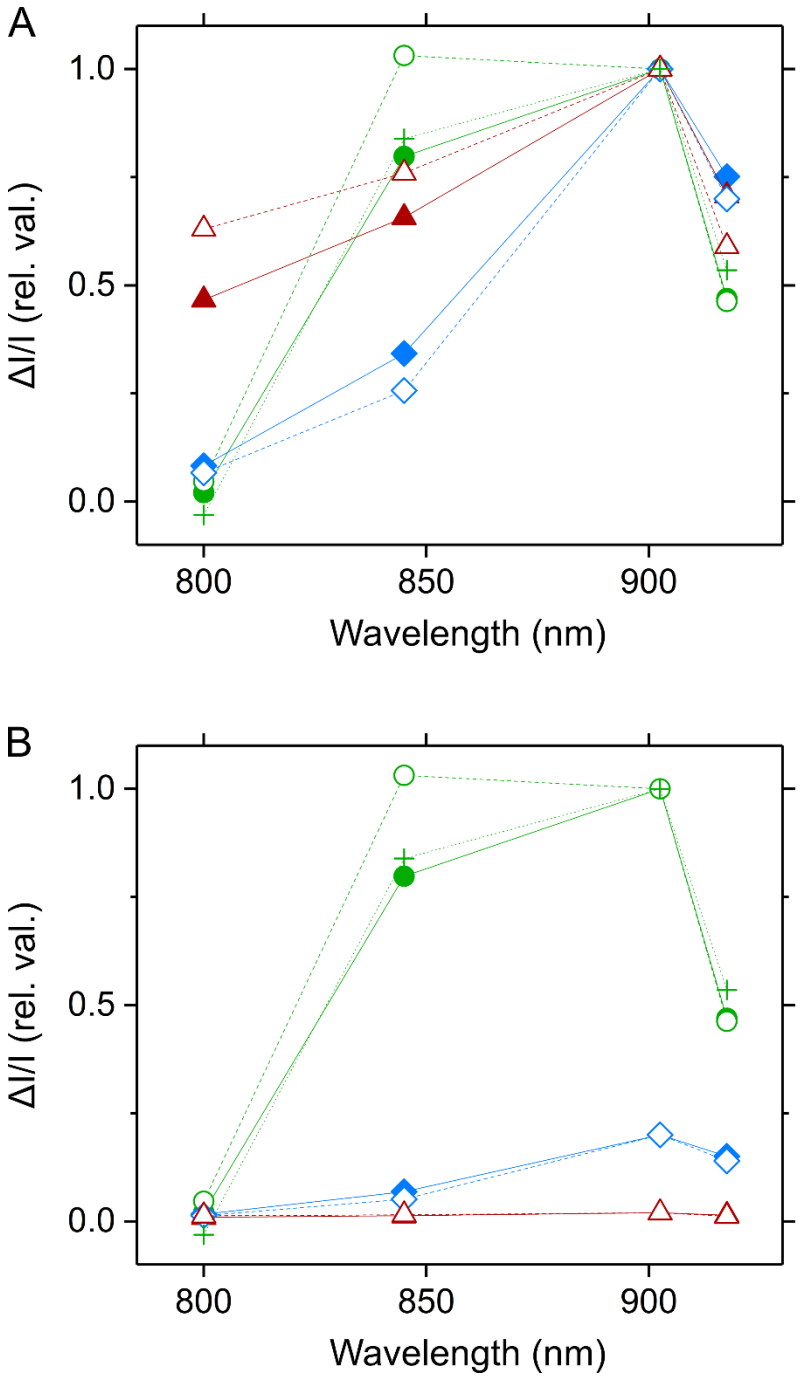

Supplemental Fig. S1. Reference model spectra in barley (closed symbols, solid lines) and *Synechocystis* sp. PCC 6803 (open symbols, dashed lines) for P700 (green circles), plastocyanin (Pcy; blue diamonds) and ferredoxin (Fd; wine red triangles). The model spectrum for P700 in *Thermosynechococcus elongatus* is shown in blue crosses (dotted line). The mean values of the transmittance differences of four wavelength pairs are shown in the central wavelength respectively. The spectra are normalized at 902.5 nm (A) and re-plotted in according to the contributions of each component to the Klas-NIR signals reported by Sétif et al. (2019) (B).